Supermode Switching in Coherently-Coupled Vertical Cavity Surface Emitting Laser Diode Arrays

Nusrat Jahan, *Student Member, IEEE,* William North, *Student Member, IEEE,* Pawel Strzebonski, *Student Member, IEEE,* and Kent D. Choquette, *Fellow, IEEE*

Abstract—We report and analyze the supermode switching with current injection found for coherently-coupled dual-element vertical cavity surface emitting laser arrays. The output power, spectral characteristics, and far-field mode profile are measured for a range of bias current operating conditions. The coupling-induced enhanced output power from an in-phase or out-of-phase supermode is confirmed when approximately equal currents are injected into each array element. We observe that the coherent supermode switches from out-of-phase to in-phase supermode with increasing equal current injection. The switching is found to be consistent with coupled mode theory and a 1-dimensional spatial supermode model. The calculated modal gain of the out-of-phase and in-phase array supermodes are consistent with the observed switching of the coherent supermodes.

Index Terms—optical coupling, semiconductor laser arrays, vertical-cavity surface emitting lasers (VCSEL)

I. Introduction

COHERENTLY-coupled phased laser diode arrays have been previously explored for generation of diffraction limited and/or high brightness beams [1]. Optically-coupled vertical cavity surface emitting laser (VCSEL) arrays [2] have shown mode engineering [3], electronic beam-steering [4], increased modulation bandwidth [5], and enhanced digital data rate [6]. When coherently coupled, a pair of VCSELs can operate in a single coherent supermode which extends into both cavities and can be classified as the out-of-phase (far-field null on axis) or in-phase (far-field maximum on axis) array supermode, respectively [7]. Herein we report and analyze the supermode switching observed for dual-element coherently-coupled photonic crystal VCSEL arrays [8] with approximately equal current injection.

Coupled mode theory was previously used to extract the complex coupling coefficient between the elements of a 2x1 VCSEL array [9]. We extend our analysis with a simple 1-dimensional antiguided supermode model [10] and show the

dominant lasing supermode should switch with increasing current injection. The output power, spectral properties, and far-field profiles are characterized for 850nm 2x1 photonic crystal VCSEL arrays. We observe the lowest threshold lasing supermode to switch from out-of-phase to in-phase with increasing current injection, consistent with the index change accompanying the increasing bias current.

Fig. 1 shows the top-view of our 2-element coupled VCSEL array. The missing holes in the photonic crystal etched in the top distributed Bragg reflector mirror denotes the two VCSEL cavities. The two VCSEL cavities are electrically isolated with multiple proton implantations in the narrow region separating the two cavities, as well as to define two circular current apertures (within the missing hole region) that have independent top anode contacts as apparent in Fig. 1. The design and fabrication of these arrays can be found in detail in Ref. [8]. By independently adjusting the bias currents injected into the two adjacent cavities, the elements can be tuned into resonance where the array operates in a coherent supermode [11]. Thus, for identical VCSEL elements, coherent supermode emission is expected with approximately equal currents in each cavity. Here we analyze a dual element array with a cavity separation of $d_c = 1.4\ \mu m$ between the left and right single-mode VCSEL elements which have a total gain area of $101\mu m^2$.
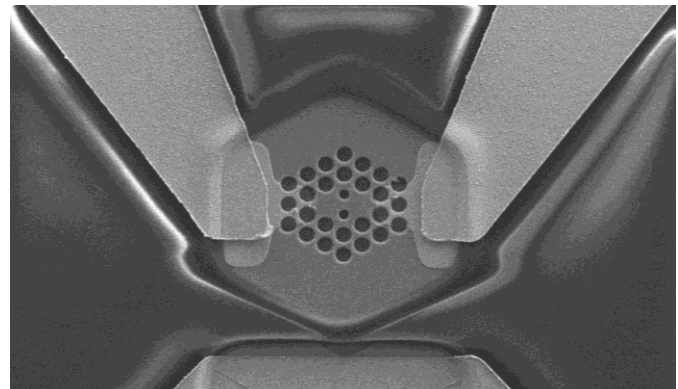

Fig. 1. Top scanning electron micrograph image of dual-element VCSEL array defined by two missing holes in the photonic crystal pattern [8]. Each cavity has separate top anode contact and common cathode.

Urbana, IL 61801 USA (e-mail: nusratj2@illinois.edu; wnorth2@illinois.edu; strzebo2@illinois.edu; choquett@illinois.edu)

II. THEORY

From the combined analysis of coupled mode theory and coupled rate equations, this system can be shown to be non-Hermitian [12] and exception point modes can be identified [13]. The strength of coupling can be quantified using a complex coupling coefficient [9]. This analysis shows that the imaginary component of the coupling coefficient corresponds to the modal gain difference between the supermodes, while the real component is related to the frequency difference between the supermodes. Furthermore, the gain of the lowest loss array supermode will be less than that of a single cavity individual mode. As a consequence, when the VCSEL array is tuned into coherent operation, an increase of the coherent array output power is observed and has recently been characterized [14].
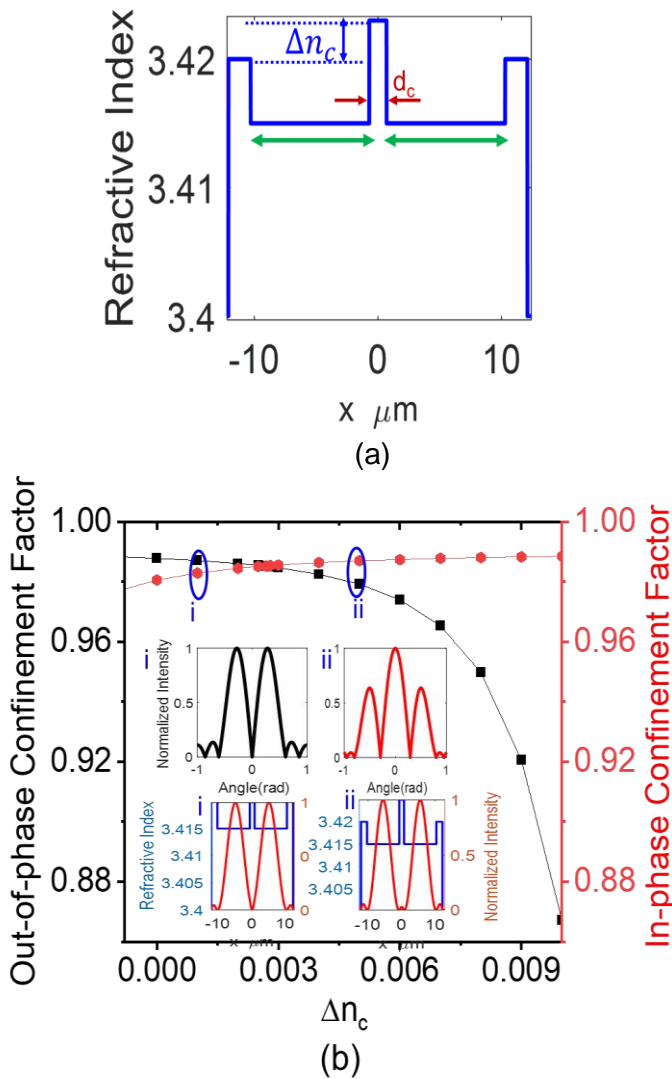

(a)

(b)

Fig. 2. (a) 1-dimensional approximate index profile of 2-element VCSEL array accounting for the thermal and carrier effects. The green arrows show the gain apertures, Δn_c is the index difference between the central implanted region and the outer cladding, d_c is the fixed separation between elements; (b) calculated confinement factor of the in-phase (circular points) and out-of-phase (square points) supermodes as a function of Δn_c. The inset shows the normalized far-field intensity and near-field mode profiles at points (i) and (ii).

A. Complex Coupling Coefficient

The dual-element photonic crystal VCSEL array has been shown to act as a non-Hermitian system with current-controlled nonuniform gain/loss [15]. The coupling between the array elements can be quantified using the complex coupling coefficient, $\kappa = \kappa_r + i\kappa_i$. The real component, κ_r expresses half the frequency splitting while the imaginary component, κ_i represents half of the difference in gain between the in-phase and out-of-phase array supermodes [9]. As noted above, coherent emission into a supermode requires less gain than the individual cavity modes; thus, when the array operation is adjusted from two independent single element lasing modes to a coherent supermode, enhanced output power, ΔP, is measured. The magnitude of the imaginary coupling coefficient, $|\kappa_i|$, scales with ΔP and the optical power of the uncoupled laser elements, $P_{uncoupled}$:

$$|\kappa_i| = \frac{\alpha_{diff}\tau_N\Delta P}{2\tau_P\left(2\hbar\omega\alpha_m V_a + \alpha_{diff}\tau_N P_{uncoupled}\right)} \quad (1)$$

where α_{diff} is the differential gain, τ_N is the carrier lifetime, τ_P is the cavity photon lifetime, α_m is the mirror loss, V_a is the active volume of the laser array [14]. These latter parameters are considered constant while ΔP and $P_{uncoupled}$ are the two experimental variables that dictate $|\kappa_i|$. The current induced variation of the refractive index causes a reversal of the power transfer and the sign of κ_i expresses that variation. When the out-of-phase supermode has lower threshold than the individual elements, and hence becomes the dominant lasing mode, κ_i is positive, and it is negative for in-phase array supermode [9]. Experimentally we can extract the magnitude of the imaginary coupling coefficient from the measured output power as a function of injected currents to the array elements [14]. We next compute κ_i using a simple one-dimensional antiguided supermode model to simulate the in-phase and out-of-phase supermodes.

B. Antiguided Supermode of VCSEL Array

We can model the supermodes arising from our 2-element VCSEL array using the leaky-mode index profile discussed in Ref. [10]. Thermal heating from increased current injection increases the refractive index, while the increased carrier density associated with this injection creates a suppression in index inside the laser cavities [16]. The two competing effects result in an antiguided index profile where the index between the laser elements is always greater than inside the laser cavities. In Fig. 2(a) we show the approximated 1-dimensional refractive index profile of the 2-elemet array. The suppressed index in the left and right gain apertures are denoted in Fig. 2(a). The index difference between the center implanted region and the cavity edge is Δn_c and the separation of the cavities is fixed to $d_c = 1.4\mu m$. Using finite difference method, we solve the Helmholtz wave equation,

$$\frac{d^2U(x)}{dx^2} + k_0^2 \, n^2(x)U(x) = n_{eff}^2 U(x) \quad (2)$$

where, n_{eff} is the effective index, k_0 is the vaccum wavenumber, and $U(x)$ is the modal field to be determined. The

anti-guided in-phase and out-of-phase supermodes are sketched in Fig. 2(b) inset. We calculate the overlap of each supermode with the gain regions (green arrows in Fig. 2(a)) to find the confinement factor shown in Fig. 2(b). With fixed cavity separation and increasing bias current to both cavities, we expect Δn_c indicated in Fig. 2(a) to monotonically increase.

For increasing Δn_c, the computed out-of-phase and in-phase supermode confinement factors are shown in Fig. 2(b). For anti-guided modes, the confinement factor of the supermodes, rather than their effective index, determines which mode has the lowest threshold gain [3]. The inset of Fig. 2(b) shows the simulated near-field and far-field profiles at two different points denoted as (i) and (ii). For this fixed cavity separation, Fig. 2(b) shows that the out-of-phase mode has the highest confinement factor for small values of Δn_c, such as shown for point (i). As Δn_c increases, the in-phase supermode confinement factor increases, while out-of-phase supermode confinement decreases, resulting in a switch of the lowest threshold supermode.

III. Experiment and Analysis

In this section, we discuss the experimental results and observations on our coherently coupled 2-element VCSEL array. The output power, near-field intensity, and far-field profile can be measured as a function of the two bias currents, which can be used to characterize the coherent properties of the arrays [5, 17]. We first identify the coherently coupled region from the enhanced output optical power as well as array emission into a single spectral peak, which occurs with approximately equal current injection into the elements. Then we analyze the supermode with increasing current by observing the resulting far-field profiles. Next, we estimate the strength of coupling by determining the imaginary coupling coefficient. Finally, we validate these results against our antiguided supermode model.

By varying the injection currents to left (I_{Left}) and right (I_{Right}) VCSEL elements, we can create 3-dimensional color contour maps to aid analysis [5, 17]. In Fig. 3(a) we present a 3-dimensional map of the measured output optical power in terms of the injection currents to the left and right laser elements, I_{Left} and I_{Right}. The color scale represents the output power at each coordinate (I_{Left}, I_{Right}). The region of power enhancement from coherent coupling is evident along the "ridge" apparent between points A and D in Fig. 3(a). This narrow region of excess power arising from the formation of the supermode corresponds to approximately equal currents injected into each element (i.e., along the diagonal in Fig. 3(a)). In Fig. 3(b) we show the spectral mapping for this array. For this measurement the number of resolvable spectral peaks above the noise floor were counted and denoted in Fig. 3(b). Notice the power ridge apparent in Fig. 3(a) also corresponds to a narrow region of apparently single mode emission. Although an apparent side mode suppression > 30 dB is measured in this region, both supermode resonances are expected within the measured single spectral linewidth.

Fig. 3(c) shows the far-field profiles measured at the points denoted in Figs 3(a) and 3(b). The far-field profiles from the apparent single spectral peak arises from dual supermode
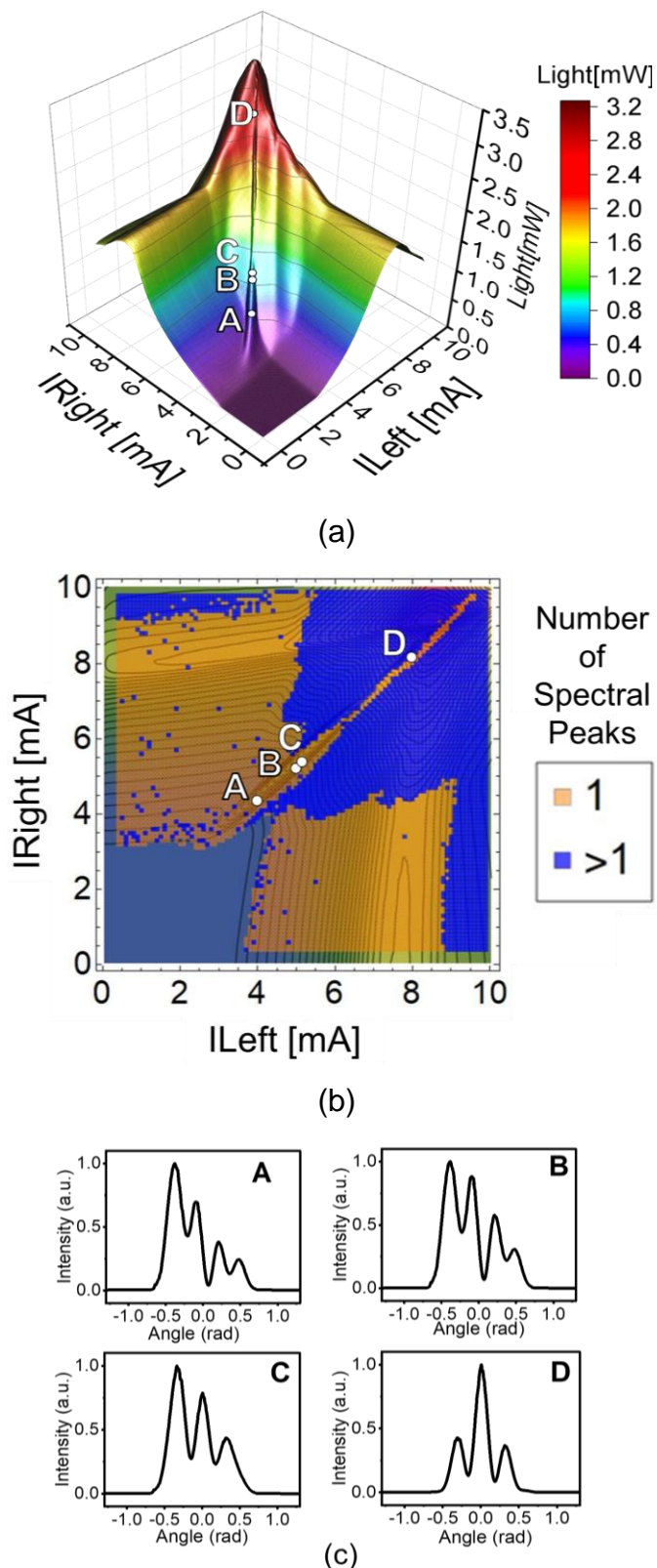

(a)

(b)

(c)

Fig. 3. Characteristics of 2-element VCSEL array: (a) 3-dimensional map of output optical power versus injection currents to the left and right elements; (b) map of the number of lasing peaks observed; and (c) selected far-field profiles measured at points A, B, C and D.
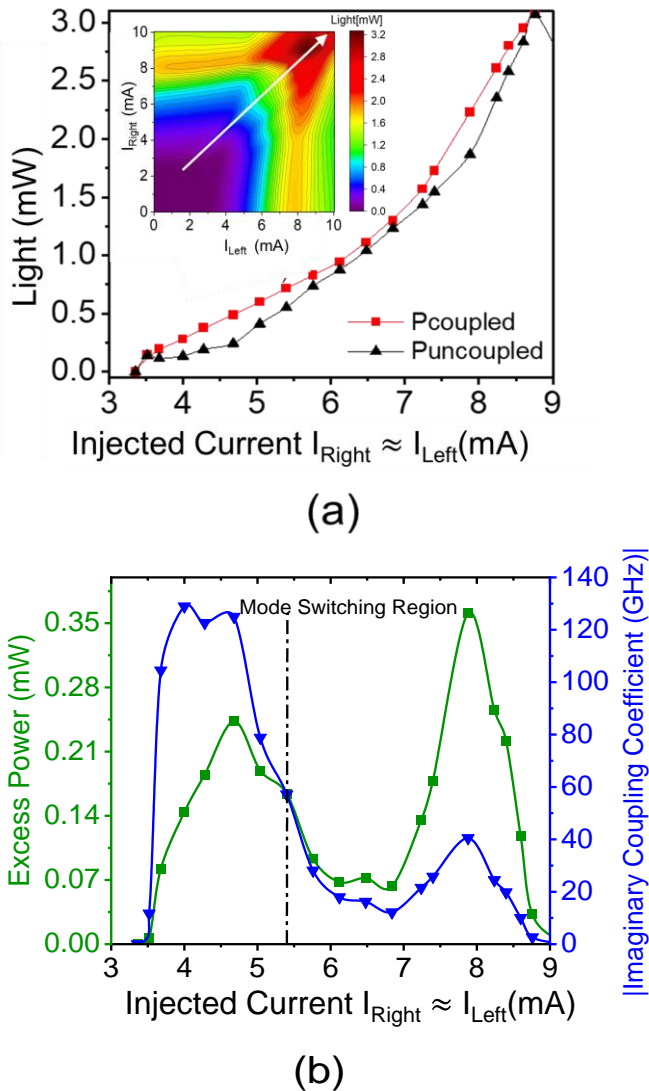
(a)

(b)

Fig. 4. (a) Uncoupled and coupled output power as a function of current, $I_{Left} \approx I_{Right}$ along the power ridge shown in inset (white arrow); (b) excess power, $\Delta P = P_{coupled} - P_{uncoupled}$, (squares) and magnitude of imaginary coupling coefficient, $|\kappa_i|$ (triangles) along the power ridge. The mode switch is marked with vertical dashed line.

emission. At point A, near threshold, the array is found to operate predominantly in the out-of-phase supermode (on axis null in far-field). With increasing approximately equal injection into each cavity (moving up the power ridge) the dominant supermode is observed to switch from the out-of-phase (points A and B) to in-phase (points C and D) supermode. The in-phase supermode (on axis maximum in far-field) remains dominant with increasing current up to the maximum array output power.

To quantify the strength of coupling, next we compute ΔP and $|\kappa_i|$ along the coupled power-ridge where $I_{Left} \approx I_{Right}$. Fig. 4(a) shows the measured coupled power, $P_{coupled}$ as well as the interpolated uncoupled power, $P_{uncoupled}$, which we estimate by fixing one current and varying the other when the currents are approximately equal. The inset of Fig. 4(a) shows how the current varies along the peak of the coherent light emission. Fig. 4(a) shows that immediately above threshold, the

coherent emission is always greater than would be measured in the absence of coupling, i.e., $P_{coupled} - P_{uncoupled} > 0$. Fig. 4(b) plots ΔP and using equation (1) plots $|\kappa_i|$ along the power ridge where $I_{Left} \approx I_{Right}$. The increase of output power from coherent coupling is seen to oscillate with increasing injection current, where a relative minimum occurs somewhat above the current where the dominant supermode emission switches. The imaginary component of coupling coefficients, $|\kappa_i|$, closely follows ΔP with increasing injection. The maximum temporal $|\kappa_i|$ computed along the power ridge is ≈ 130 GHz which decreases by an order of magnitude at the point of minimum ΔP. The dominant supermode switching occurs in between the relative maxima of $|\kappa_i|$, marked using the dash line in Fig 4(b). Since the out-of-phase supermode is observed at threshold, we know that $\kappa_i > 0$ and after the supermode switches to in-phase, κ_i is negative [9, 14].

Supermode switching and bistability in 2-element coherent VCSEL arrays has been previously noted [15, 17]. The simple anti-guided supermode model and the expected change in the index profile across the array as current is injected, described in the previous section, explains this mode switching phenomenon. The change in the modal gain of the in-phase and out-of-phase array supermode is an outcome of the index profile that varies with current injection and thus influences the overall coherent coupling.

IV. CONCLUSION

We characterize the coherent coupling of our dual-element photonic crystal VCSEL array from extensive measurements of the output optical power, spectral content, and far-field profiles versus injection currents into both elements. The far-field interference patterns show the resulting supermodes arising from the coherent coupling between the two laser elements switches from predominantly out-of-phase to in-phase with increasing injection of current along the coherently coupled power ridge (corresponding to roughly equal injection currents into each cavity). This switching involves changes in the coupling induced excess power and the corresponding imaginary component of the coupling coefficient. This supermode switching is consistent with a model of the expected coherent mode changes with varying current injection. The quantification of coherent coupling will enable further control of the dynamic properties of these arrays for emerging applications.

REFERENCES

[1] D. Botez, *Diode laser arrays*. Cambridge: Cambridge University Press, 1994.

This article has been accepted for publication in a future issue of this journal, but has not been fully edited. Content may change prior to final publication. Citation information: DOI 10.1109/JSTQE.2021.3117236, IEEE Journal of Selected Topics in Quantum Electronics

5

[2] D. F. Siriani and K. D. Choquette, "Coherent Coupling of Vertical-Cavity Surface-Emitting Laser Arrays," *Advances in Semiconductor Lasers*, pp. 227–267, 2012.

[3] B. J. Thompson, Z. Gao, S. T. Fryslie, and K. D. Choquette, "Mode Engineering in Linear Coherently Coupled Vertical-Cavity Surface-Emitting Laser Arrays," *IEEE Journal of Selected Topics in Quantum Electronics*, vol. 25, no. 6, pp. 1–5, 2019.

[4] M. T. Johnson, D. F. Siriani, M. Peun Tan, and K. D. Choquette, "Beam steering via resonance detuning in coherently coupled vertical cavity laser arrays," *Applied Physics Letters*, vol. 103, no. 20, p. 201115, 2013.

[5] S. T. Fryslie, M. P. Siriani, D. F. Siriani, M. T. Johnson, and K. D. Choquette, "37-GHz Modulation via Resonance Tuning in Single-Mode Coherent Vertical-Cavity Laser Arrays," *IEEE Photonics Technology Letters*, vol. 27, no. 4, pp. 415–418, 2015.

[6] H. Dave, P. Liao, S. T. Fryslie, Z. Gao, B. J. Thompson, A. E. Willner, and K. D. Choquette, "Digital Modulation of Coherently-Coupled 2 x 1 Vertical-Cavity Surface-Emitting Laser Arrays." *IEEE Photonics Technology Letters* 31, no. 2 pp. 173-176, 2018.

[7] G. Hadley, "Modes of a two-dimensional phase-locked array of vertical-cavity surface-emitting lasers", *Optics Letters*, vol. 15, no. 21, p. 1215, 1990.

[8] S. T. Fryslie, Z. Gao, H. Dave, B. J. Thompson, K. Lakomy, S. Lin, P. J. Decker, D. K. McElfresh, J. E. Schutt-Aine, and K. D. Choquette, "Modulation of Coherently Coupled Phased Photonic Crystal Vertical Cavity Laser Arrays," *IEEE Journal of Selected Topics in Quantum Electronics*, vol. 23, no. 6, pp. 1–9, 2017.

[9] Zihe Gao, "Non-Hermitian aspects of coherently coupled vertical cavity laser arrays" *PhD thesis, University of Illinois at Urbana-Champaign,* 2018.

[10] D. F. Siriani and K. D. Choquette, "Implant Defined Anti-Guided Vertical-Cavity Surface-Emitting Laser Arrays," *IEEE Journal of Quantum Electronics*, vol. 47, no. 2, pp. 160–164, 2011.

[11] S. Fryslie, M. Johnson and K. Choquette, "Coherence Tuning in Optically Coupled Phased Vertical Cavity Laser Arrays", *IEEE Journal of Quantum Electronics*, vol. 51, no. 11, pp. 1-6, 2015.

[12] Z. Gao, M. Johnson and K. Choquette, "Rate equation analysis and non-Hermiticity in coupled semiconductor laser arrays", *Journal of Applied Physics*, vol. 123, no. 17, p. 173102, 2018.

[13] Z. Gao, B. Thompson, H. Dave, S. Fryslie and K. Choquette, "Non-Hermiticity and exceptional points in coherently coupled vertical cavity laser diode arrays", *Applied Physics Letters*, vol. 114, no. 6, p. 061103, 2019.

[14] H. Dave, Z. Gao, and K. Choquette, "Complex coupling coefficient in laterally coupled microcavity laser diode arrays," *Applied Physics Letters*, vol. 117, no. 4, p. 041106, 2020.

[15] Z. Gao, S. T. Fryslie, B. J. Thompson, P. S. Carney, and K. D. Choquette, "Parity-time symmetry in coherently coupled vertical cavity laser arrays," *Optica*, vol. 4, no. 3, p. 323, 2017.

[16] N. Dutta, L. Tu, G. Hasnain, G. Zydzik, Y. Wang and A. Cho, "Anomalous temporal response of gain guided surface emitting lasers", *Electronics Letters*, vol. 27, no. 3, p. 208, 1991.

[17] H. Dave, Z. Gao, S. T. M. Fryslie, B. J. Thompson, and K. D. Choquette, "Static and Dynamic Properties of Coherently-Coupled Photonic-Crystal Vertical-Cavity Surface-Emitting Laser Arrays," *IEEE Journal of Selected Topics in Quantum Electronics*, vol. 25, no. 6, pp. 1–8, 2019.

Nusrat Jahan (GSM'17) received B.S. and M.S. degrees in Electrical and Electronic Engineering from Bangladesh University of Engineering and Technology (BUET). She is currently working towards a Ph.D. degree in electrical engineering at the University of Illinois at Urbana-Champaign. Her main research interests are characterization and analysis of coherently coupled photonic crystal VCSEL arrays.

William North received B.S. degree in Electrical Engineering from the United States Military Academy (USMA) and M.S. degree in Electrical Engineering from Stanford University, CA. He is currently working towards a Ph.D. degree in electrical engineering at the University of Illinois at Urbana-Champaign. His main research interests are high-speed and high-power photonic crystal VCSEL coupled arrays.

Pawel Strzebonski Pawel Strzebonski received the B.S. degree in electrical engineering, the M.S. and Ph.D. degrees in electrical and computer engineering from the University of Illinois, Urbana-Champaign, Urbana, IL, USA, in 2016, 2018, and 2021, respectively. His main research interests include computational methods for the design and characterization of various photonic devices, including photonic crystal VCSEL arrays and photonic crystal surface emitting lasers.

Kent D. Choquette (M'97–F'03) received B.S. degrees from the University of Colorado-Boulder, Boulder, CO, USA, and the M.S. and Ph.D. degrees from the University of Wisconsin-Madison, USA. He held a postdoctoral appointment at AT&T Bell Laboratories, Murray Hill, NJ, USA and joined Sandia National Laboratories in Albuquerque, NM, USA. He joined the Electrical and Computer Engineering Department at the University of Illinois and is currently the Able Bliss Professor of Engineering. He leads the Photonic Device Research Group which pursues the design, fabrication, characterization, and applications of semiconductor vertical cavity surface-emitting lasers, photonic crystal light sources, nanofabrication technologies, and hybrid integration techniques. He has authored more than 500 technical publications and presentations at international conferences.

Dr. Choquette received the 2008 IEEE Photonics Society Engineering Achievement Award, the 2012 OSA Nick Holonyak Jr. Award, and the 2016 SPIE Technology Achievement award. He is a Fellow of IEEE, the Optical Society, SPIE, and the American Association for the Advancement of Science.